Structure and Gas Sorption Behavior of a New Three Dimensional Porous Magnesium Formate

(Supporting Information: 21 pages including this page)

Arijit Mallick, Subhadeep Saha, Pradip Pachfule, Sudip Roy and Rahul Banerjee*

Physical/Materials Chemistry Division, National Chemical Laboratory, Dr. Homi Bhaba Road, Pune- 411008, India
E-mail: r.banerjee@ncl.res.in Fax: + 91-20-25902636; Tel: + 91-20-25902535

Section S1: Detailed synthesis procedures for *γ*-Mg-formate including multi-gram scale products, experimental and simulated PXRD patterns:

1,3-benzeneditetrazole, $Mg(COOCH_3)_2 \cdot 4H_2O$ were purchased from the Aldrich Chemicals. *N*, *N*-dimethylformamide (DMF) was purchased from Rankem chemicals. All starting materials were used without further purification. All experimental operations were performed in air.

Synthesis of *γ*-Mg-formate $Mg_3(O_2CH)_6 \supset [NH(CH_3)_2]_{0.5}$: As 1,3-benzeneditetrazole is sparingly soluble in water at moderate temperature. So we used the solvent DMF in which it is readily soluble. So we used the solvothermal condition (teflon-lined stainless steel autoclave at 125 to 150 $^{\circ}$C) for synthesis which results into the formation of single crystals suitable for X-ray diffraction. Before solvothermal reactions, stirring of the heterogeneous solutions for a period of 30 minutes was helpful for the high purity of the product. Solvothermal reaction of $Mg(CO_2CH_3)_2 \bullet 4H_2O$ (0.214 g, 1 mmol) with 1,3-benzeneditetrazole (0.214 g, 1 mmol) in a 25 ml Teflon-lined stainless steel autoclave in 5 ml DMF and 0.2 ml HNO_3 (3.6 M) mixture at 150 $^{\circ}$C for 60 h produces colorless crystals of $Mg_3(O_2CH)_6 \supset [NH(CH_3)_2]_{0.5}$ in 61% yield. Crystals were collected by filtration and dried in air (10 min). [Yield: 61%, 0.130 gm depending on $Mg(CO_2CH_3)_2 \bullet 4H_2O$]. ***FT-IR*** **:** (KBr 4000-400cm^{-1}): 3302(br), 2906(w), 1683(w), 1598(s), 1404(m), 1375(m), 1364(m), 841(w), 761(w), 694(w), 574(w). Elemental Analysis: Calculated- C (23.20%), H (0.82%), N (1.93%); Found C (21.20%), H (0.72%), N (2.03%).

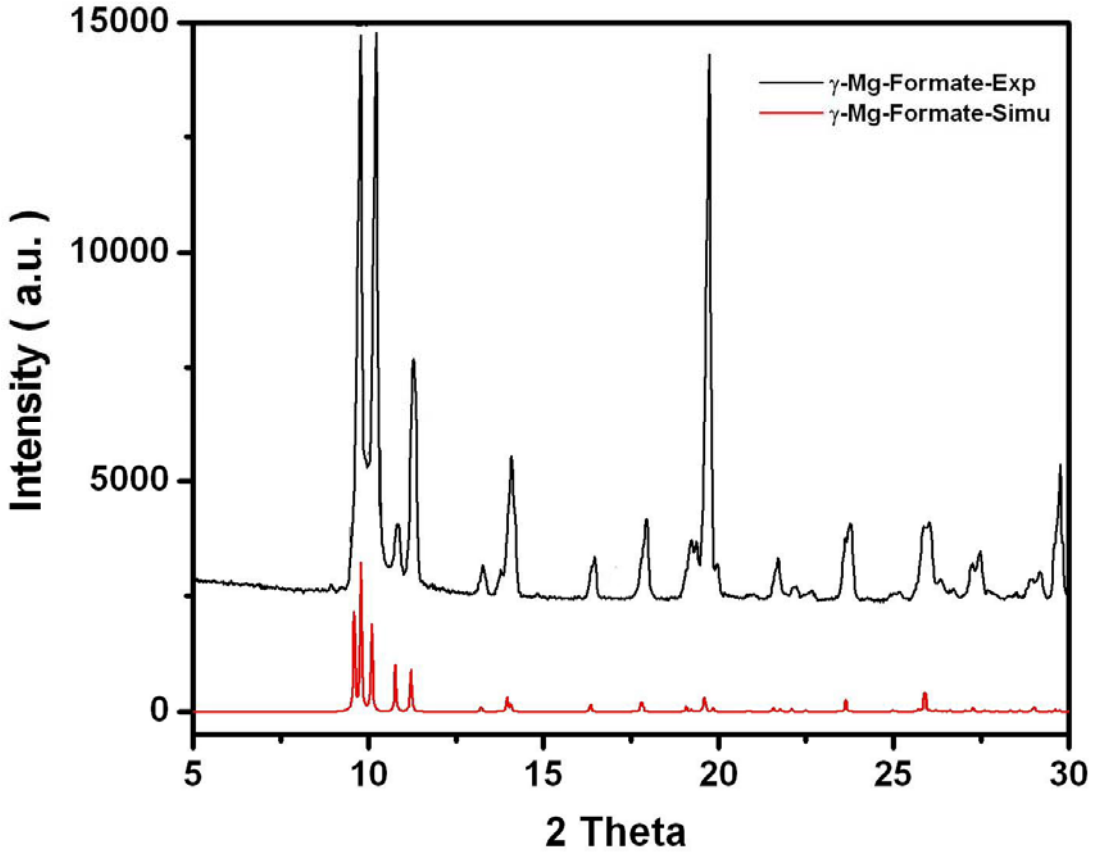

Figure S1. Comparison of the experimental PXRD pattern of as-synthesized *γ*-Mg-formate (top) with the one simulated from its single crystal structure (bottom).

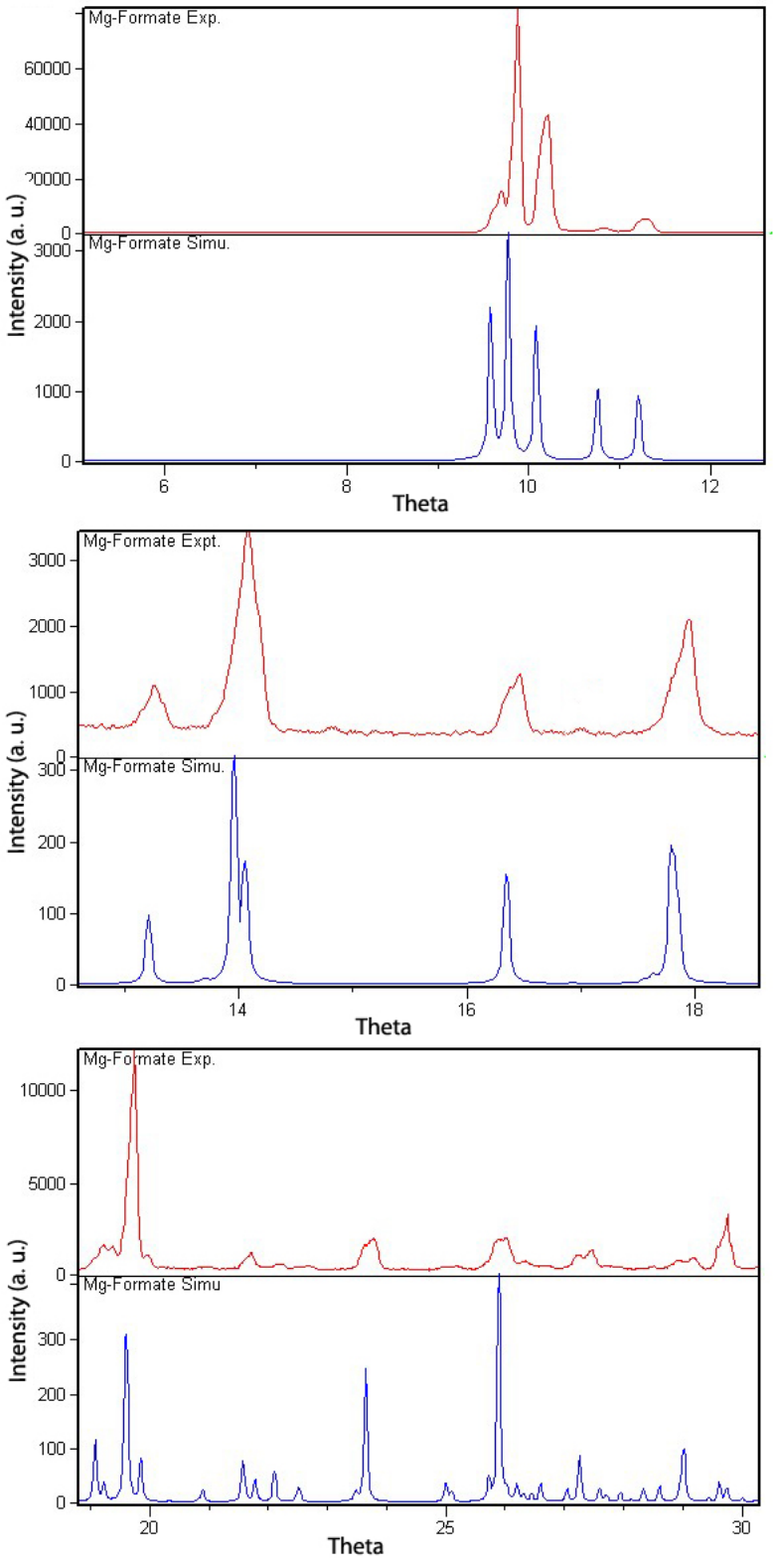

Figure S2. Enlarge picture of comparison of the experimental PXRD pattern of as-synthesized γ-Mg-formate with the simulated from its single crystal structure.

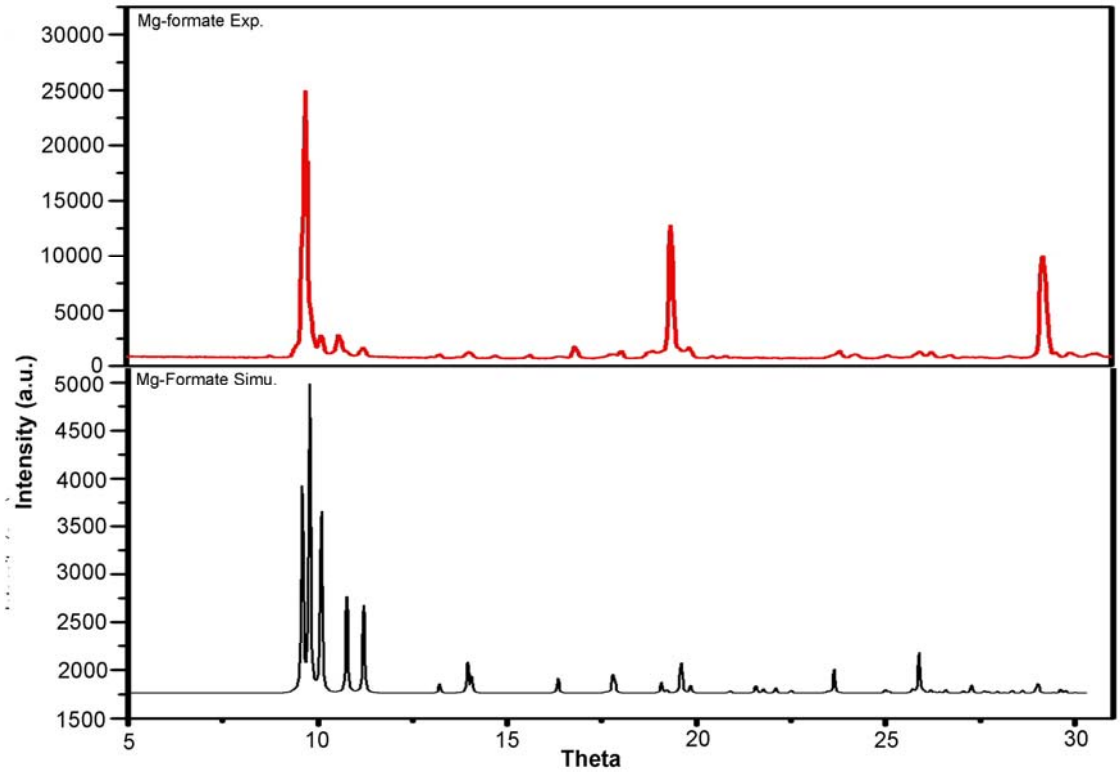

Figure S3. Comparison of the experimental PXRD pattern of evacuated *γ*-Mg-formate (top) with the one simulated from its single crystal structure (bottom).

Section S2. Single crystal X-ray diffraction data collection, structure solution and refinement procedures.

General Data Collection and Refinement Procedures:

The single crystal data was collected on a Bruker SMART APEX three circle diffractometer equipped with a CCD area detector and operated at 1500 W power (50 kV, 30 mA) to generate Mo Kα radiation (λ=0.71073 Å). The incident X-ray beam was focused and monochromated using Bruker Excalibur Gobel mirror optics. Crystal of the γ-Mg-formate reported in the paper was mounted on nylon CryoLoops (Hampton Research) with Paraton-N (Hampton Research). Crystals were flash frozen to 293(2) K in a liquid nitrogen cooled stream of nitrogen.

Initial scans of each specimen were performed to obtain preliminary unit cell parameters and to assess the mosaicity (breadth of spots between frames) of the crystal to select the required frame width for data collection. In this case frame widths of 0.5° was judged to be appropriate and full hemispheres of data were collected using the *Bruker SMART*[1] software suite. Following data collection, reflections were sampled from all regions of the Ewald sphere to re-determine unit cell parameters for data integration and to check for rotational twinning using CELL_NOW[2]. In no data collection was evidence for crystal decay encountered. Following exhaustive review of the collected frames the resolution of the dataset was judged. Data was integrated using Bruker SAINT [3] software with a narrow frame algorithm and a 0.400 fractional lower limit of average intensity. Data was subsequently corrected for absorption by the program SADABS[4]. The space group determinations and test for merohedral twinning was carried out using *XPREP*[3]. In this case, the highest possible space group was chosen.

The structure was solved by direct method and refined using the *SHELXTL 97*[5] software suite. Atoms were located from iterative examination of difference F-maps following least squares refinements of the earlier models. Final model was refined anisotropically (if the number of data permitted) until full convergence was achieved. Hydrogen atoms were placed in calculated positions (C-H = 0.93 Å) and included as riding atoms with isotropic displacement parameters 1.2-1.5 times U_{eq} of the attached C atoms. In some cases modeling of electron density within the voids of the frameworks did not lead to identification of recognizable solvent molecules in these structures, probably due to the highly disordered contents of the large pores in the frameworks. Highly porous crystals that contain solvent-filled pores often yield raw data where observed strong (high intensity) scattering becomes limited to ~1.0 Å at best, with higher resolution data present at low intensity. A common strategy for improving X-ray data, increasing the exposure time of the crystal to X-rays, did not improve the quality of the high angle data in this case, as the intensity from low angle data saturated the detector and minimal improvement in the high angle data was achieved. Additionally, diffused scattering from the highly disordered solvent within the void spaces of the framework and from the capillary to mount the crystal contributes to the background and the 'washing out' of the weaker data. The only optimal crystals suitable for analysis were generally small and weakly diffracting. Unfortunately, larger crystals, which would usually improve the quality of the data, presented a lowered degree of crystallinity and attempts to optimize the crystal growing conditions for large high-quality specimens have not yet been fruitful. Data were collected at 298(2) K for the MOF presented in this paper. This lower temperature was considered to be optimal for obtaining the best data. Electron density

within void spaces has not been assigned to any guest entity but has been modeled as isolated oxygen and/or carbon atoms. The foremost errors in all the models are thought to lie in the assignment of guest electron density. The structure was examined using the *Adsym* subroutine of PLATON[7] to assure that no additional symmetry could be applied to the models. The ellipsoids in ORTEP diagrams are displayed at the 50% probability level unless noted otherwise. For all structures we note that elevated R-values are commonly encountered in MOF crystallography for the reasons expressed above by us and by other research groups.[8-17] Table S1 contains crystallographic data for the γ-Mg-formate.

1. Bruker (2005). *APEX2*. Version 5.053. Bruker AXS Inc., Madison,Wisconsin, USA.
2. Sheldrick, G. M. (2004). *CELL_NOW*. University of Göttingen, Germany. Steiner, Th. (1998). *Acta Cryst*. B54, 456–463.
3. Bruker (2004). *SAINT-Plus* (Version 7.03). Bruker AXS Inc., Madison, Wisconsin, USA.
4. Sheldrick, G. M. (2002). *SADABS* (Version 2.03) and *TWINABS* (Version 1.02).University of Göttingen, Germany.
5. Sheldrick, G. M. (1997). *SHELXS '97* and *SHELXL '97*. University of Göttingen, Germany.
6. WINGX
7. A. L. Spek (2005) PLATON, *A Multipurpose Crystallographic Tool*, Utrecht University, Utrecht, The Netherlands.

8. L. A. Dakin, P. C. Ong, J. S. Panek, R. J. Staples, and P. Stavropoulos, *Organometallics,* 2000, **19**, 2896.

9. S. Noro, R. Kitaura, M. Kondo, S. Kitagawa, T. Ishii, H. Matsuzaka, and M. Yamashita, *J. Am. Chem. Soc.* 2002, **124**, 2568.

10. M. Eddaoudi, J. Kim, D. Vodak, A. Sudik, J. Wachter, M. O'Keeffe, and O. M. Yaghi, *Proc. Natl. Acad. Sci. USA,* 2002. **99**, 4900.

11. R. A. Heintz, H. Zhao, X. Ouyang, G. Grandinetti, J. Cowen, and K. R. Dunbar, *Inorg. Chem.* 1999, **38**, 144.

12. K. Biradha, Y. Hongo, and M. Fujita, *Angew. Chem. Int. Ed.* 2000, **39**, 3843.

13. P. Grosshans, A. Jouaiti, M. W. Hosseini, and N. Kyritsakas, *New J. Chem, (Nouv. J. Chim,)* 2003, **27**, 793.

14. N. Takeda, K. Umemoto, K. Yamaguchi, and M. Fujita, *Nature (London)* 1999, **398**, 794.

15. M. Eddaoudi, J. Kim, N. Rosi, D. Vodak, J. Wachter, M. O'Keeffe, and O. M. Yaghi, *Science,* 2002, **295**, 469.

16. B. Kesanli, Y. Cui, M. R. Smith, E. W. Bittner, B. C. Bockrath, and W. Lin, *Angew. Chem. Int. Ed,.* 2005, **44,** 72.

17. F. A. Cotton, C. Lin, and C. A. Murillo, *Inorg. Chem.* 2001, **40**, 478.

γ-Mg-formate (Orthorhombic)

Experimental and Refinement Details for *γ*-Mg-formate

A colorless prismatic crystal (0.20 × 0.16 × 0.12 mm^3) of *γ*-Mg-formate was placed in a 0.7 mm diameter nylon CryoLoops (Hampton Research) with Paraton-N (Hampton Research). The loop was mounted on a SMART APEX three circle diffractometer. A total of 2830 reflections were collected of which 1417 were unique and 1000 of these were greater than 2σ (*I*). The range of θ was from 2.47 to 25.97º. All non-hydrogen atoms were refined anisotropically. *γ*-Mg-formate contains six formate anion and three metal atom in the asymmetric unit. It should be noted that other supporting characterization data (*vide infra* Section S1) are consistent with the crystal structure. Final full matrix least-squares refinement on F^2 converged to $R_1 = 0.0687$ ($F > 2\sigma F$)) and $wR_2 = 0.1257$ (all data) with GOF = 0.937.

Table S1. Crystal data and structure refinement for *γ*-Mg-formate

Empirical formula	$C_{14}H_{12}Mg_6NO_{24}$
Formula weight	724.11
Temperature	293(2)K
Wavelength	0.71073Å
Crystal system	Orthorhombic
Space group	*P*bcn
Unit cell dimensions	*a* = 9.9638(18)Å α = 90.00°
	b = 18.450(3)Å β = 90.00°
	c = 18.082(3)Å γ = 90.00°
Volume	3324.1(10) $Å^3$
Z	4
Density (calculated)	1.447 Mg/m^3
Absorption coefficient	0.236
F(000)	1468
Crystal size	0.20 × 0.16 × 0.12 mm^3
Theta range for data collection	2.47- 25.97
Index ranges	-11<= h <= 11, -21<= k <= 21, -21<= l <= 21
Reflections collected	2830
Independent reflections	1417
Completeness to theta = 26.02°	100 %
Absorption correction	Semi-empirical from equivalents
Refinement method	Full-matrix least-squares on F^2
Data / restraints / parameters	2830 / 0 / 198
Goodness-of-fit on F^2	0.937
Final R indices [I>2sigma(I)]	R_1 = 0.0687, , wR_2 = 0.1257
R indices (all data)	R_1 = 0.1337, , wR_2 = 0.1567
Largest diff. peak and hole	0.900 and -0.400e.$Å^{-3}$

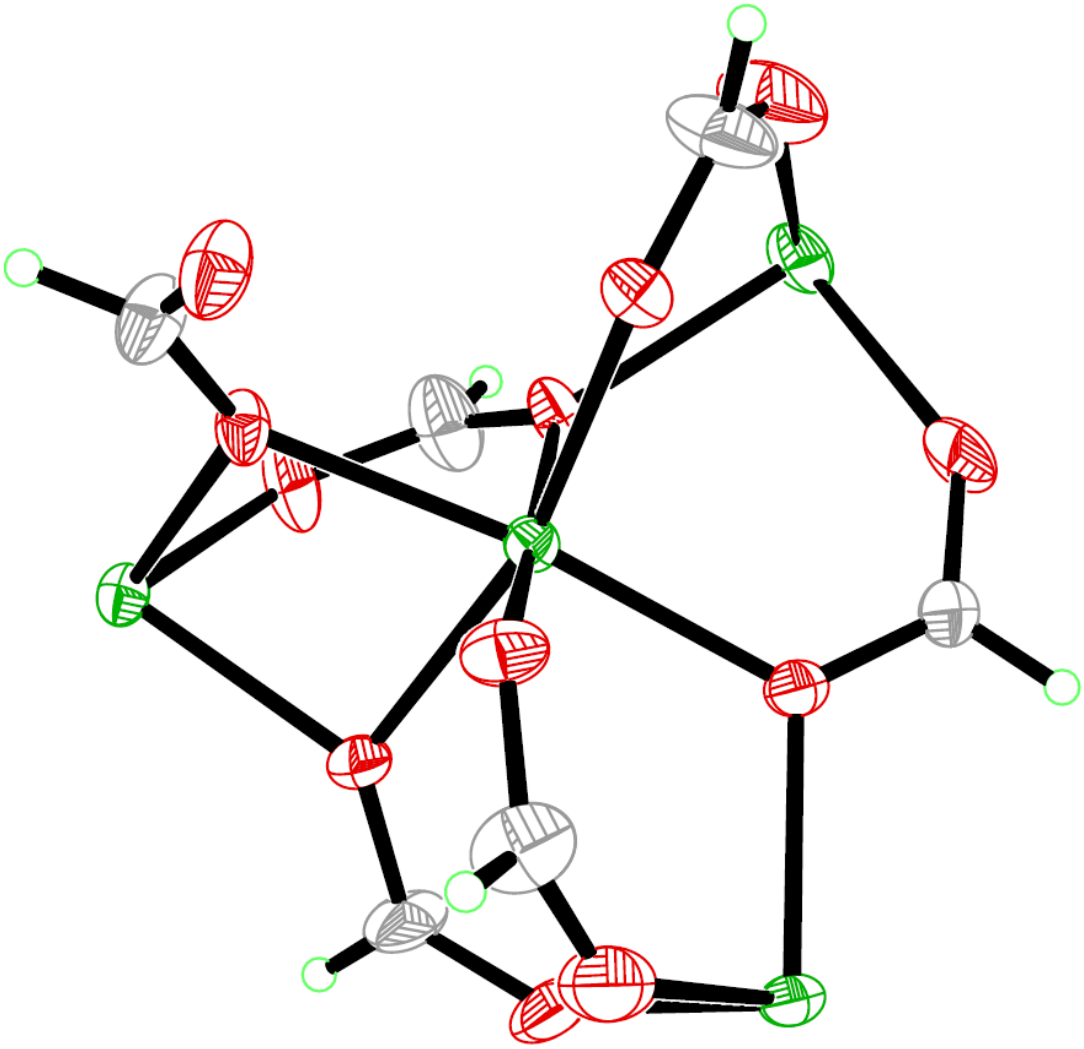

Figure S4. ORTEP drawing of the asymmetric unit of γ-Mg-formate.

Section S3. Thermal stability of *γ*-Mg-formate:

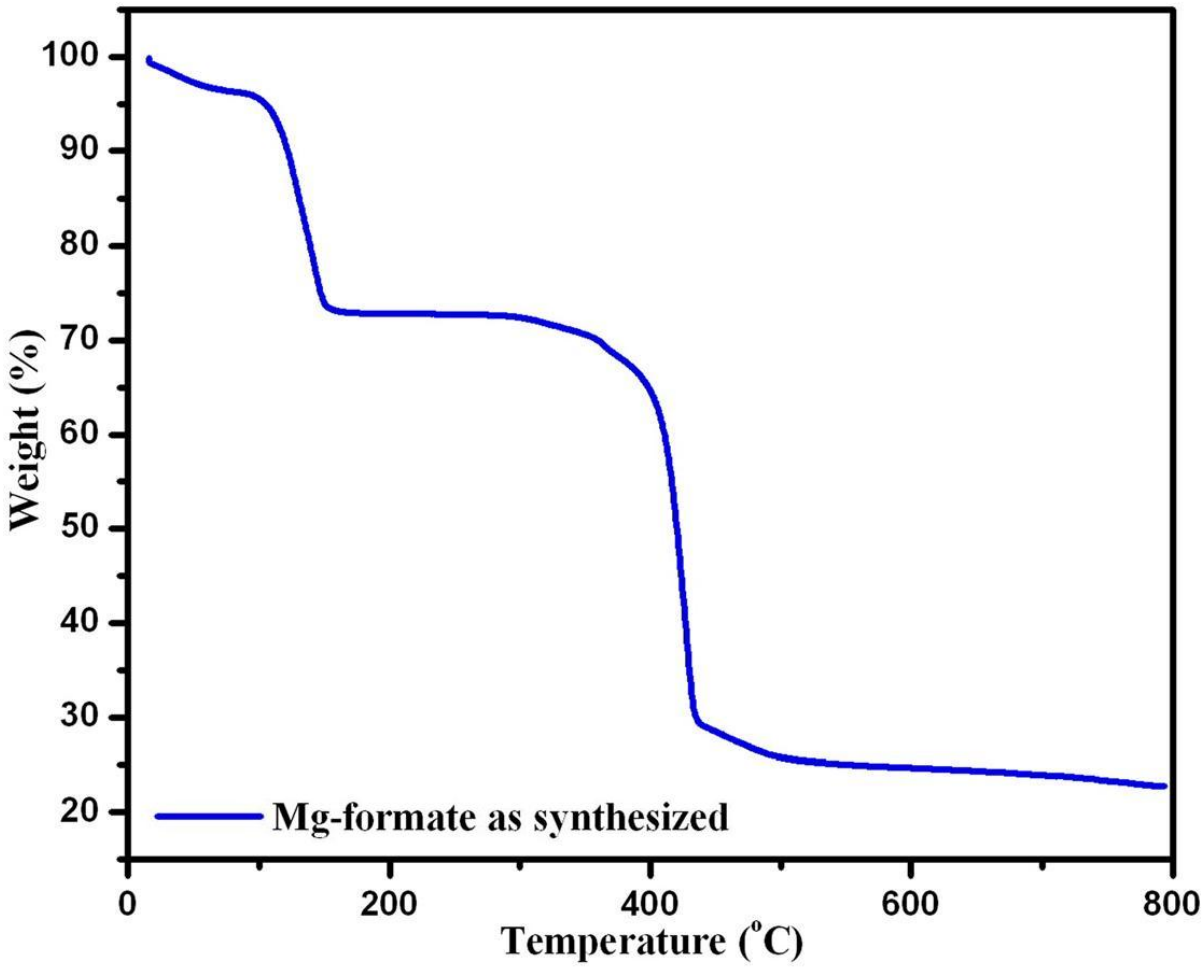

Figure S5: Thermo gravimetric analysis (TGA) plot of *γ*-Mg-formate.

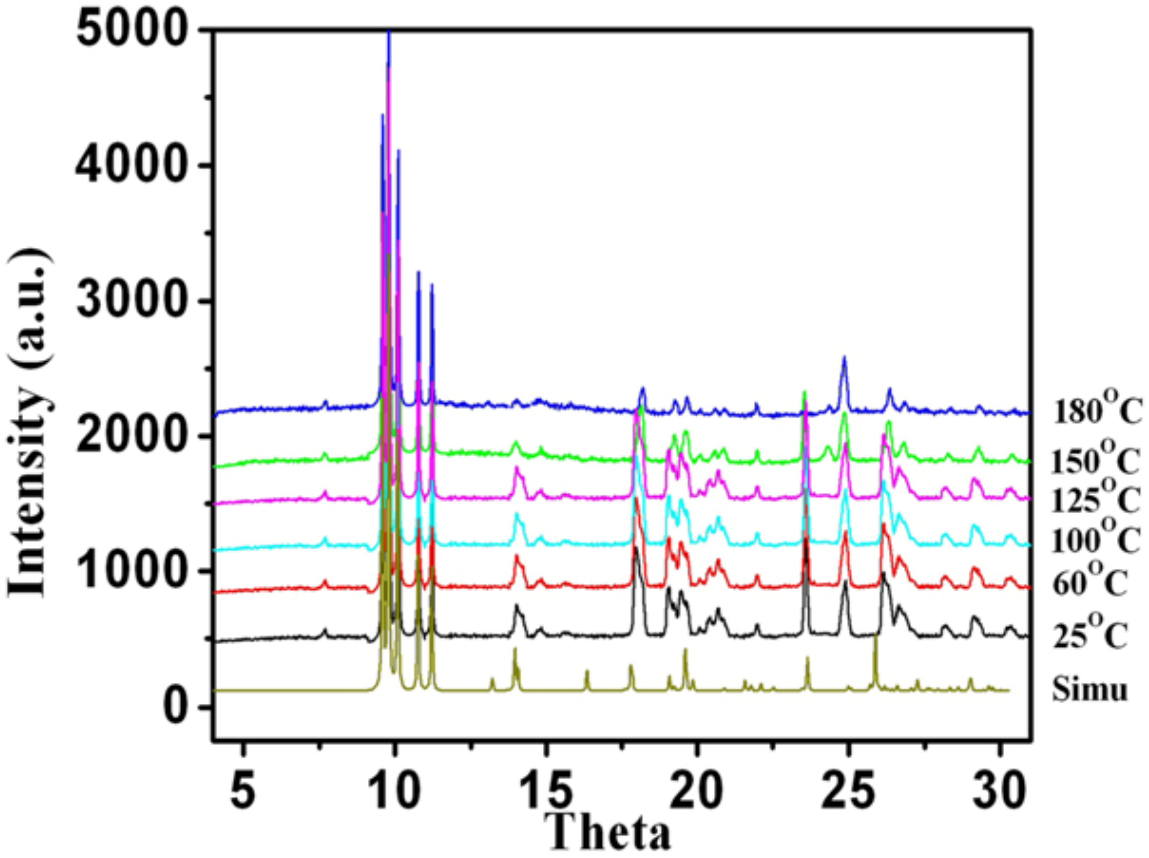

Figure S6: VTPXRD for γ-Mg-formate.

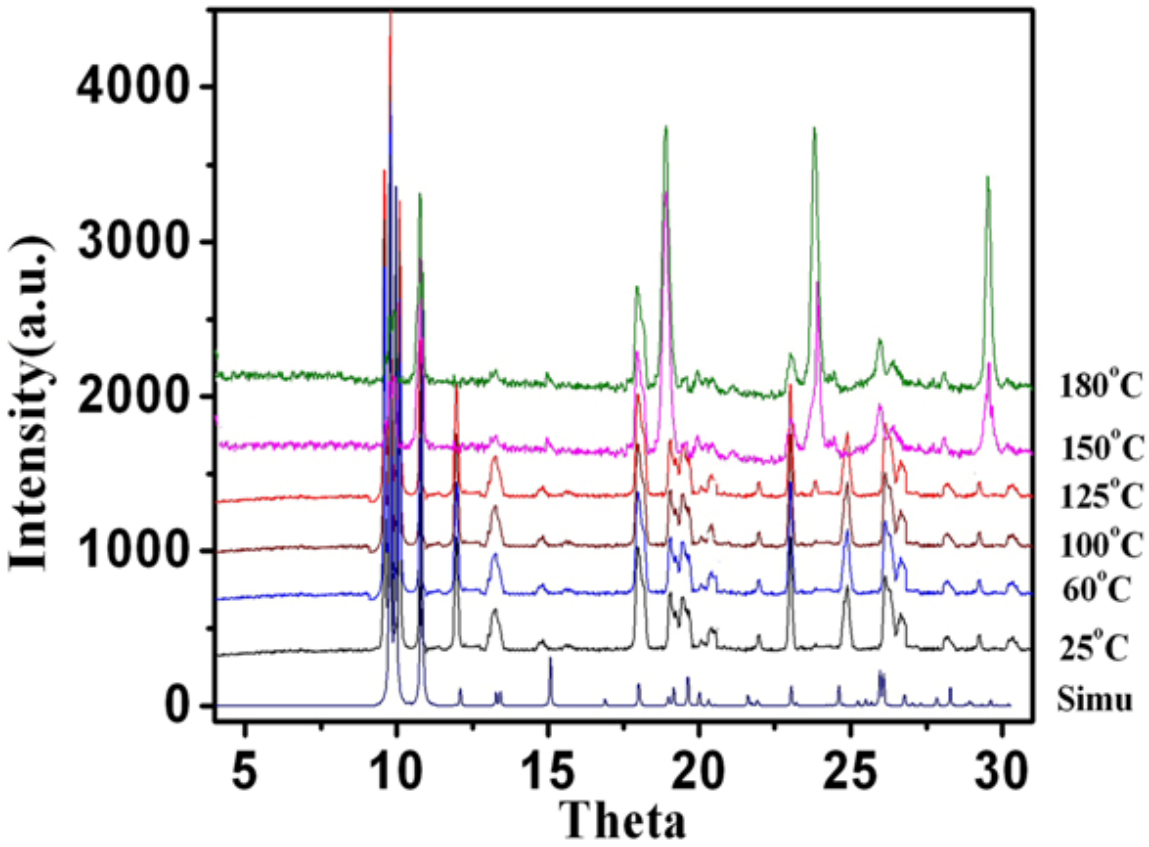

Figure S7: VTPXRD for α-Mg-formate**.**

Table S2. CO_2 uptake (mmol/g) of different MOFs at 298K with references.

SL. No.	MOF	CO2 uptake* mmol/g	Reference
1	Mg\DOBDC	8.08	J. Am. Chem. Soc. 2008, 130, 10870
2	Co\DOBDC	7.1	J. Am. Chem. Soc. 2008, 130, 10870
3	Bio MOF 11	6.0	J. Am. Chem. Soc**.** 2010, 132, 38
4	Ni\DOBDC	5.8	J. Am. Chem. Soc**.,**2008, 130, 10870
5	Zn\DOBDC	5.5	J. Am. Chem. Soc**.,** 2008, 130, 10870
6	HKUST-1 [$Cu_3(BTC)_2(H_2O)_4$]	4.6	Microporous and Mesoporous Materials, 2002, 55, 217
7	Zn + 4,4' bipy + (BTA-TBA)	4.1	J. Am. Chem. Soc**.,** 2010, 132, 950
8	$Zn_2(C_2O_4)(C_2N_4H_3)_2.(H_2O)_{0.5}$	3.78	Chem. Commun., 2009, 5230
9	UMCM-150	2.8	J. Am. Chem. Soc**.,** 2007, 129, 15740
10	SNU- M10 ($[(Ni_2L^2)(bptc)]\cdot 6H_2O\cdot 3DEF$)	2.1	Angew. Chem. Int. Ed. 2009, 48, 6865
11	IMOF-3($C_6H_6N_4O_2Zn$)	2.14	Angew. Chem. Int. Ed. 2010, 49, 1258
12	α-Mg formate ($Mg_3(O_2CH)_6$)	1.7	Chem. Asian J. 2007, **2**, 484.
13	SNU-25, $MgC_{40}H_{28}N_2O_{10}$	1.48	Chem. Commun., 2009, 5436
14	$C_{45}H_{52}N_4O_{17}Zn_2$,	1.36	Chem. Commun., 2010, 46, 538
15	$C_{58}H_{38}N_4O_{16}Zn_2$	1.07	Chem. Eur. J. 2010, 16, 276

*All CO_2 uptakes at 1 bar and 298 K.

1. Stephen R. Caskey, Antek G. Wong-Foy, and Adam J. Matzger, *J. Am. Chem. Soc.* 2008, **130**, 10870.
2. Stephen R. Caskey, Antek G. Wong-Foy, and Adam J. Matzger, *J. Am. Chem. Soc.* 2008, **130**, 10870.
3. J. An, S. J. Geib, and N. L. Rosi, *J. Am. Chem. Soc***.,** 2010, **132**, 38.
4. Stephen R. Caskey, Antek G. Wong-Foy, and Adam J. Matzger, *J. Am. Chem. Soc.* 2008, **130**, 10870.

5. Stephen R. Caskey, Antek G. Wong-Foy, and Adam J. Matzger, *J. Am. Chem. Soc.* 2008, **130**, 10870.

6. Q. M. Wang, D. Shen, M. B€ulow, M. L. Lau, S. Deng, F.R. Fitch, N. O. Lemcoff, J. Semanscin, Microporous and Mesoporous Materials, 2002, **55**, 217.

7. O. K. Farha, C. D. Malliakas, M. G. Kanatzidis, and J. T. Hupp, *J. Am. Chem. Soc***.** 2010, **132**, 950.

8. R. Vaidhyanathan, S. S. Iremonger, K. W. Dawson, and G. K. H. Shimizu, *Chem. Commun*., 2009, 5230.

9. A. G. Wong-Foy, O. Lebel, and A. J. Matzger, *J. Am. Chem. Soc.,* 2007, **129**, 15740.

10. H.-S. Choi and M. P. Suh, *Angew. Chem. Int. Ed*. 2009, **48**, 6865.

11. F. Debatin, A. Thomas, A. Kelling, N. Hedin, Z. Bacsik, I. Senkovska, S. Kaskel, M. Junginger, H. Mller, U. Schilde, C. J_ger, A. Friedrich, and H.-J. Holdt, *Angew. Chem. Int. Ed*. 2010, **49**, 1258.

12. D. G. Samsonenko, H. Kim, Y. Sun, G.-H. Kim, H.-S. Lee, and K. Kim, *Chem. Asian J*. 2007, **2**, 484.

13. Y. E. Cheon, J. Park and M. P. Suh, *Chem. Commun*., 2009, 5436.

14. M. Radha Kishan, J. Tian, P. K. Thallapally, C. A. Fernandez, S. J. Dalgarno, J. E. Warren, B. P. McGraila and J. L. Atwood, *Chem. Commun*., 2010, **46**, 538.

15. K. L. Mulfort, O. K. Farha, C. D. Malliakas, M. G. Kanatzidis, and J. T. Hupp, Chem. Eur. J. 2010, **16**, 276.

.

Table S3. CO_2 uptake (mmol/g) of different Mg-MOFs at 298K with references.

SL. No.	MOF	CO2 uptake* mmol/g	Reference
1	Mg\DOBDC	8.08	J. Am. Chem. Soc. 2008, 130, 10870
2	α-Mg formate ($Mg_3(O_2CH)_6$)	1.7	Chem. Asian J. 2007, **2**, 484.
3	SNU-25, $MgC_{40}H_{28}N_2O_{10}$	1.48	Chem. Commun., 2009, 5436
4	$Mg(HCOO)_3@(CH_3)_2NH$	0.3	Crystal Growth and Design, 2008, **8**, 3302

*All CO_2 uptakes at 1 bar and 298 K.

1. S. R. Caskey, A. G. Wong-Foy, and Adam J. Matzger, *J. Am. Chem. Soc.* 2008, **130**, 10870.
2. Y. E. Cheon, J. Park and M. P. Suh, *Chem. Commun*., 2009, 5436.
3. A. Rossin, A. Ienco, F. Costantino, T. Montini, B. D. Credico, M. Caporali, L. Gonsalvi, P. Fornasiero, and Maurizio Peruzzini, *Crystal Growth and Design,* 2008,**8**, 3302.
4. D. G. Samsonenko, H. Kim, Y. Sun, G.-H. Kim, H.-S. Lee, and K. Kim, *Chem. Asian J.* 2007, **2**, 484.
5. D. Britt, H. Furukawa, B. Wang, T. G. Glover, and O. M. Yaghi, *Proc. Natl. Acad. Sci.*, 2009, **106**, 20637.

Section S4. Computational Studies on *γ*-Mg-formate.

Computational procedures.

Introduction. In this work apart from the synthesis and experimental characterization ab-initio quantum chemical study (DFT) has been performed on the finite structure of α -formate and *γ*-Mg-formate. To build MOF based materials with high gas storage capacity it is essential to have a molecular level understanding of interactions. The storage capacity of different types of gases at different temperatures is strongly dependent upon the interactions between the MOF framework and gas molecules. The measure of this interaction is the adsorption energy between the framework and gas molecules. Low adsorption energies e.g. lower than -10 KJ/mol attribute to weak interaction and leads to physisorption. Whereas adsorption energies higher than these may lead to stronger interactions hence better binding to the framework,i.e, chemisorption. Finding the adsorption sites in the framework and their energies will also produce valuable information about the amount of the intake of gas molecules. If the adsorption energy is much higher at a particular site of the pore (e.g. near to the metal center) than other sites then the number of adsorbed gas molecules will be more at that particular site. Therefore first principle quantum chemistry calculations are useful to scan the adsorption sites and their respective adsorption energies to predict the adsorption capacity and further tuning the chemistry of the framework. In this study we have used grand canonical Monte Carlo (GCMC) simulation using the to predict the initial positions of the hydrogen molecules in the framework and ab-initio Density Functional Theory (DFT) method to optimize the positions of the each hydrogen molecules in the framework and their related adsorption energies.

Initial structure generation. Selection of initial positions of hydrogen molecules in the framework is the most important step for calculating the probable binding sites and the corresponding binding energy. Proper scanning of pore surface is important to get the adsorption site with the highest binding energy. It is difficult to find homogeneously distributed initial positions of hydrogen molecules in the framework due to the 3 dimensional structure of the MOF. Even if we find homogeneously distributed positions, executing calculations for all the initial structure means large number of optimization calculations. Therefore, we choose the initial structure from the output of our classical grand canonical Monte Carlo simulation, which we have performed for calculating adsorption isotherms.

The conventional GCMC simulation technique is used to compute adsorption isotherms. The input for the simulation consists of models (structures) for the adsorbent and the adsorbate as well as force fields which describe the interactions between them. MOFs are crystalline therefore model for the adsorbent in the atomistic representation of the framework is taken from its crystallographic coordinates. Here, for γ–Mg-formate we have used the original crystal structure ignoring the solvent molecule residing in the pore. In all the simulations, the framework is treated as rigid (a valid assumption for many MOFs at low temperature), although models for flexible MOFs have been proposed recently. We have calculated the theoretical gas adsorption isotherm for γ–formate and α-formate. In order to avoid boundary or finite size effects and to allow simulations that are valid for the extended crystal lattice, periodic boundary conditions has been used, resulting in simulations that take place in an infinite, perfect structure. To model adsorbate/adsorbate and adsorbate/framework interactions, van der Waals interactions

(normally modelled by Lennard-Jones potentials) have been taken into account. Lennard-Jones (LJ) parameters for the individual atoms and for H_2 molecule UFF potential parameters has been considered. LJ potential parameters for cross interactions were computed from Lorentz–Berthelot combining rules. The cutoff radii for both the MOFs were set to be 4.8 Å. For GCMC calculations the volume (V), the temperature (T) and the chemical potential (μ) are kept fixed and under these conditions, the average number of molecules adsorbed is computed. Each step in the Monte Carlo routine consisted of the insertion of a new molecule, deletion of an existing molecule, or translation of an existing molecule. A total of 5 million steps were used, the first half for equilibration and the second half to calculate the ensemble averages. A configuration is defined as an attempted translation, rotation, creation or deletion of a H_2 molecule. The probability of attempting creation or deletion of a molecule was set to 0.3 an equation of state for hydrogen was used to obtain the relationship between the bulk pressure and fugacity. We have converted the total adsorption obtained from simulation to excess adsorption to compare with the experiments. The details of the conversion calculations can be found in the literature. Along with the adsorption isotherm the positions (coordinates) of the adsorbed hydrogen molecules in the pores of both of α and γ-Mg-formate were obtained. Finite structures (shown in figure S6) of the frameworks have been generated with different positions of hydrogen molecules. These initial structures were further optimized by ab-initio quantum chemical calculations.

Calculation of adsorption energy and site. Finite structure obtained from the periodic structure possesses artificial dangling bonds. We have saturated those bonds with H atoms. For geometry optimization Gaussian 09 software suite has been used. The

ModRedundant option has been employed to perform the selective optimization of H atoms which have been attached to the clusters to saturate the dangling bonds at the B3LYP/6-31G level of theory to get the energy, $E_{(BAREMOF)}$ of the finite structure. Hydrogen molecule on the finite structure was inserted at the same positions that we obtained from GCMC simulation. Then we have optimized the positions of hydrogen molecules of each initial structure containing finite formate clusters (α-formate and γ–Mg-formate both) and one hydrogen molecule using density functional theory (DFT) with 6-31G basis set. The energies we calculated from these calculations are for adsorbate-adsorbent complex, $E_{(BAREMOF+H2)}$. We have determined the binding energy of hydrogen using the following equation, where $E_{(H2)}$ is the energy of H_2 molecule obtained from DFT calculation with the same basis set.

$E_{ads} = E_{(BAREMOF+H2)} - (E_{(BAREMOF)}+E_{(H2)})$

Adsorption energies after optimization of all initial configurations for each type of MOFs were compared. The lowest adsorption energies refer to the positions of the hydrogen molecules in the pores and reported in the paper.

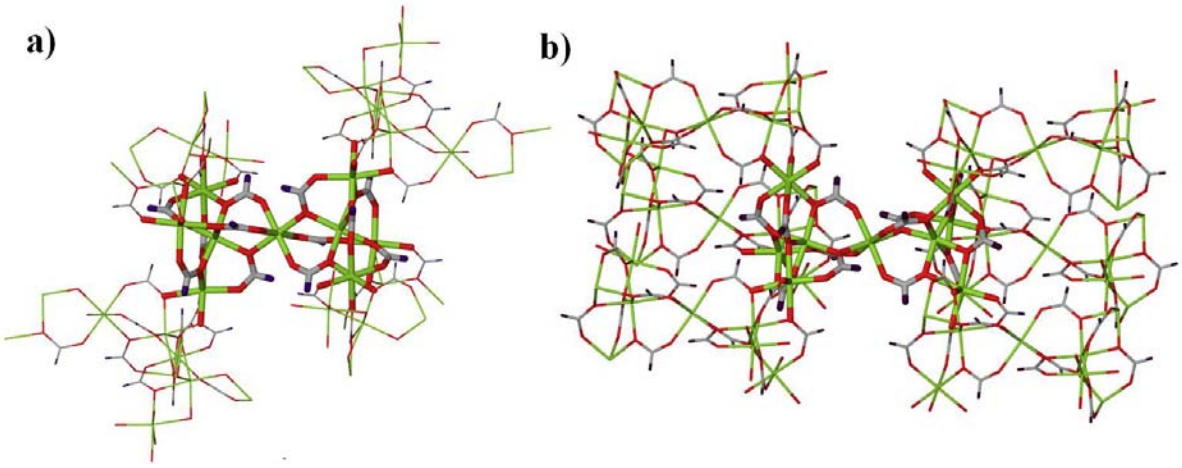

Figure S8: : Highlighted region shows the region extracted from the 111 supercell of (a) α-Mg-formate, (b) γ-Mg-formate.for quantum chemical calculation.